

Electronic structure and bonding in ternary Zintl phases: LiAlSi

N. E. Christensen

Max-Planck-Institut für Festkörperforschung, D-7000 Stuttgart 80, Federal Republic of Germany

(Received 28 May 1985)

The volume dependence of the total energy of LiAlSi compounds in three hypothetical cubic $cF12$ structures with $F\bar{4}3m$ symmetry are calculated within the local-density approximation. Predictions of structural stability agree with observations. The bonding in the stable structure, where Al and Si form a zinc-blende substructure and Li and Al are arranged in a NaCl substructure, is characterized by strong covalent Al—Si bonds. The band structure is very similar to that of pure Si. Trends in the calculated physical properties of the series, Si, LiAlSi, LiAl, are discussed. Structural phase transitions and insulator-metal-insulator transitions in LiAlSi under pressure are predicted.

I. INTRODUCTION

Silicon, which at ambient conditions assumes the diamond structure, is the most studied and important representative of the tetrahedrally bonded semiconductors. The crystal structure, and a schematic representation of the bonds, are shown in Fig. 1, if it is assumed that Si atoms occupy the sites labeled *A* and *C*, and that the sites *B* and *D* are vacant. The intermetallic compound LiAl crystallizes in the $B32$ structure, which may be considered as derived from that of Si by replacing the Si atoms (*A* and *C*) in Fig. 1 by aluminium and introducing Li on the positions *D* and *B*. According to the chemical picture of Zintl and Brauer¹ the stability of LiAl (and of a number of related compounds) in this phase is explained in terms of a transfer of the $2s$ electron from Li to Al which then can form covalent sp^3 bonds as found in Si. Indeed recent calculations² showed that LiAl has a band structure which, apart from a small band overlap, is similar to that of Si. Furthermore, it was found² that the bonding, at least qualitatively, is quite well described by the original model.¹ If this is true, it is natural to assume that a stable, related compound can be derived from Si by replacing only *half* of the Si atoms, those on the *A* sites by Al and placing Li on *either* *D* or *B* (Fig. 1). In view of the chemical picture referred to above, we should expect such a compound to exist, and to have electronic and cohesive properties similar to those of Si. Indeed, a ternary LiAlSi compound does exist,³ and we shall here present first-principles calculations of total energies for three different (hypothetical) cubic structures. The most stable structure can be selected, and furthermore, pressure-induced phase transitions will be discussed. The nature of the bonding will be discussed in terms of calculated electron distributions and the similarities with Si will become obvious.

II. METHOD OF CALCULATION

Total energies are here calculated within the local-density approximation (LDA) to the density-functional formalism.⁴⁻⁷ The band structure, i.e., the self-consistent solutions of the Schrödinger-like single-particle equation,

is obtained by means of Andersen's linear-muffin-tin-orbital (LMTO) method.⁸ Relativistic effects are included, except for the spin-orbit coupling; i.e., we use the so-called "scalar-relativistic" scheme. The "combined correction term"⁸ is included. This is particularly important for some of the conduction states in the tetrahedral semiconductors.⁹⁻¹¹ Figure 2 shows the band structure of Si in the LDA. The top of the valence bands is Γ'_{25} and the gap is indirect, Γ'_{25} to Δ_1 (near *X*). The value of the calculated gap (≈ 0.7 eV) is smaller than observed, as is always the case when the LDA eigenvalues are compared to experimental⁹⁻¹² data for conduction states in insulators. The volume for which the band structure in Fig. 2 was calculated corresponds to an average atomic-sphere radius¹³ $S_{av} = 2.526$ a.u. This is the experimental equilibrium volume as well as that corresponding theoretically to zero pressure.

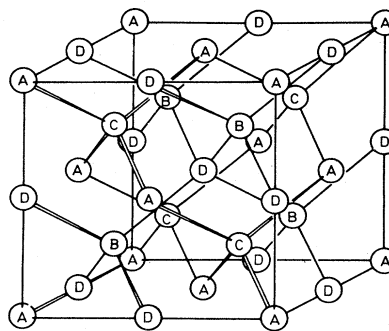


FIG. 1. Sketch of a class of cubic crystal structures based on an fcc Bravais lattice. The basis contains four atoms, *A*, *B*, *C*, and *D* at $(0,0,0)$, $(1,1,1)a/4$, $(-1,-1,-1)a/4$, and $(1,1,1)a/2$. The diamond structure corresponds to the case where *A* and *C* are occupied by identical atoms and *B* and *D* are vacant. In structure I of AlSiLi (see text), Si sits on *C*, Al sits on *A*, Li sits on *D*, and the *B* sites are empty.

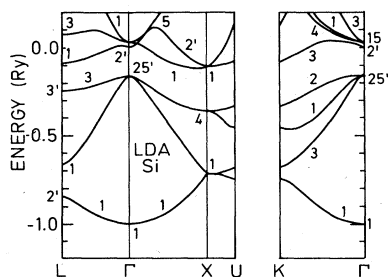


FIG. 2. Band structure of Si in the local-density approximation, i.e., the (formal) one-electron energies obtained by solving the Schrödinger-like equation with the self-consistent potential using the scalar relativistic LMTO method.

III. BAND STRUCTURES OF LiAlSi AND RELATED COMPOUNDS

The band structures of the ternary LiAlSi compounds were calculated for three structures, $\text{Al}\square\text{SiLi}$ (I), $\text{AlLiSi}\square$ (II), and $\text{LiAlSi}\square$ (III). The symbol \square means a vacant site, and technically in connection¹³ with the LMTO method an “empty sphere.” These structures are all based on the structure shown in Fig. 1, but the occupations of the sites are different (Table I). Structure I is the one which is reported³ to be stable at ambient conditions. The observed lattice constant corresponds to $S_{\text{av}}=2.7588$ a.u. We show, in Figs. 3–5, the LDA band structures for the three LiAlSi structures all calculated for a volume ($S_{\text{av}}=2.8$ a.u.) close to the observed. It is seen (Figs. 3 and 4) that I ($\text{Al}\square\text{SiLi}$) and II ($\text{AlLiSi}\square$) have band structures which *both* are very similar to that of Si (Fig. 2). They are both semiconductors; the nature of the gap is in both cases the same as in Si, i.e., the indirect¹⁴ $\Gamma'_{25}\rightarrow\Delta_1$ gap. The value of the gap (in the LDA) is smaller (≈ 0.1 eV) than for pure Si (0.7 eV, Fig. 2). This is fully in agreement with what would be expected from the arguments by Zintl and Brauer, cf. Sec. I. The two structures, I and II (Table I and Fig. 1) have identical relative arrangements of the Al and Si atoms; they form in both cases a zinc-blende structure which favors for the formation of the covalent Al—Si sp^3 bonds. This condition is the main factor in the formation of the semiconducting electronic structure. The actual position of the Li atom is less important in that respect. Whether it sits on a *D* site (I) or a *B* site (II) can hardly affect the band structure.^{15,16}

TABLE I. Three structures of LiAlSi considered. The upper site labels refer to Fig. 1. Those given below give the Wyckoff positions. The open square means “vacant” [and in the LMTO calculations these positions are treated as atoms with $Z=0$ (see also Ref. 13)].

	A 4a	B 4c	C 4d	D 4b
$\text{Al}\square\text{SiLi}$ (I)	Al	\square	Si	Li
$\text{AlLiSi}\square$ (II)	Al	Li	Si	\square
$\text{LiAlSi}\square$ (III)	Li	Al	Si	\square

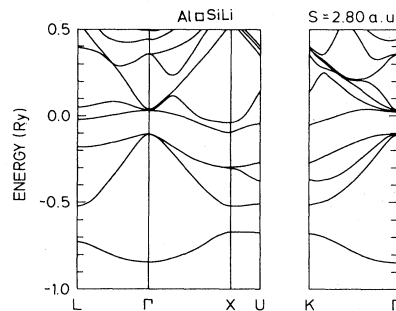


FIG. 3. LDA band structure of LiAlSi in structure I (cf. Table I and Fig. 1). The volume corresponds to the average atomic-sphere radius (Ref. 13) $S_{\text{av}}=2.80$ a.u., i.e., the lattice is slightly expanded with respect to the observed equilibrium volume ($S_{\text{av}}=2.7588$ a.u.).

The third (hypothetical) structure examined here, III, differs from I and II in the relative Al-Si positions. This structure is the one which mostly resembles that of CaF_2 , from which it may be derived by placing Li on the Ca positions. The arrangement of the aluminum and silicon atoms in this case does not allow the formation of Al—Si sp^3 bonds. The band structure (Fig. 5) shows no gap, i.e., $\text{LiAlSi}\square$ is a metal.

The similarities between the electronic structures of Si and the two semiconducting structures I and II of LiAlSi can also be illustrated by calculation of total and partial density-of-states functions (Figs. 6–10). Only some of the projected density of states (DOS) are shown. The results, Figs. 6 and 7, for pure Si serve as a “reference.” The Si *s* and Si *p* DOS in $\text{Al}\square\text{SiLi}$ (I) (Figs. 8 and 9) have essentially the same shapes and magnitudes as those in pure Si. The Al *p* DOS is also qualitatively very similar, but the amplitudes are smaller. This (Fig. 9) is also seen in the integrated function [the Al *p* number of states (NOS)]. The valence states of LiAlSi in structure I contain in the present model^{17,18} ≈ 0.5 Al *p* electrons less than the number of *p* electrons per Si site. This reflects¹⁷ the fact that although our basic picture of the bonding in AlSiLi suggests sp^3 covalent bonding between Al and Si, the bonding is less complete or “weaker” than in Si.

The compound LiAl, formed by replacing all Si atoms

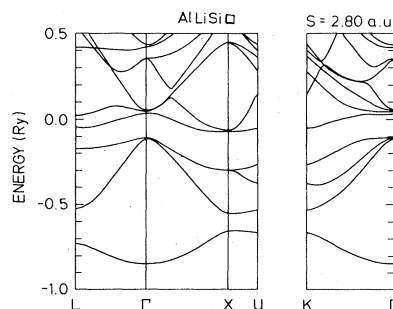


FIG. 4. Band structure of $\text{AlLiSi}\square$ (II). $S_{\text{av}}=2.80$ a.u.

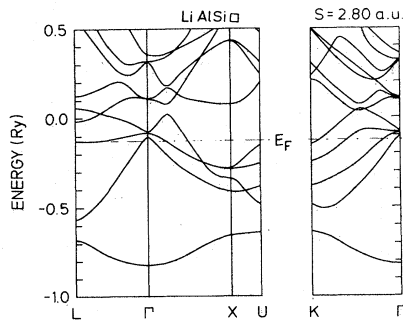


FIG. 5. Band structure of $\text{LiAlSi}\square$ (III). $S_{\text{av}}=2.80$ a.u.

by Al, also has² similarities with Si and AlSiLi . For a comparison of the band structures the reader is referred to Ref. 2. Here, we include (Figs. 11 and 12) the calculated density of states. Although LiAl is a metal, the DOS functions still are similar to those of Si. The gap is closed, but the band overlap (the X_1^c level lies¹⁴ below Γ_{25}') is small. Thus, the DOS has a low value near E_F . Figures 6–12 thus on one hand illustrate the similarities in bonding, but on the other hand they also show a smooth trend in the sequence $\text{Si} \rightarrow \text{LiAlSi} \rightarrow \text{LiAl}$ from strong to weaker covalent bonding and to bonding with clearer metallic character (Ref. 2).

IV. METALLIZATION UNDER PRESSURE

In the present work we only discuss AlSiLi in the three structures of Table I. This means that we do not, in our total-energy calculations (Sec. V), examine in detail whether the compound under pressure can assume other crystal structures, as observed for Si for example. Within

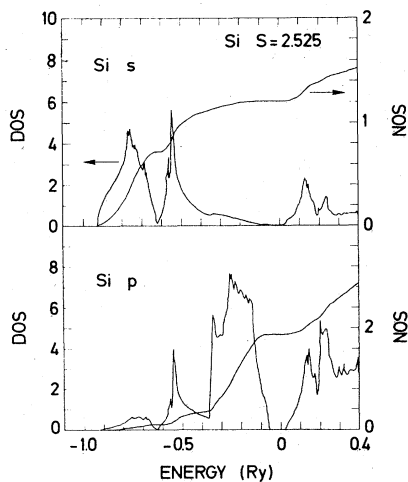


FIG. 6. Partial density-of-states (DOS) functions for Si ($S_{\text{av}}=2.526$ a.u.). Only the Si s and Si p DOS are shown. Empty-sphere contributions as well as Si d states are included in the total functions (Fig. 7). The partial number of states (NOS) is also shown (right-hand scale).

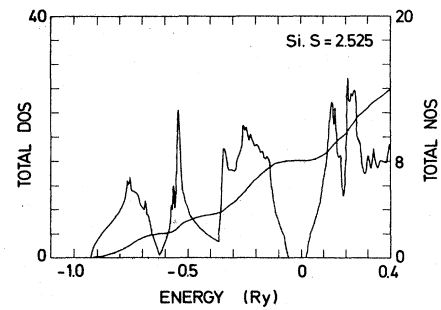


FIG. 7. Total density-of-states function for Si (DOS) and number of states (NOS). The LDA gap is 0.7 eV. (Low-density “tails” are not clearly seen in this plot which therefore appears to indicate a larger gap. See also the upper part of Fig. 6.)

the structures examined here, we find that both semiconductor phases, I and II, under pressure exhibit a transition (isostructural) to metallic phases. The pressure-induced insulator-metal transition in structure I and II is similar to the *compositional* transition occurring when going from LiAlSi to LiAl . The metallic phase occurs when the X_1^c level drops down below the valence band top¹⁴ (Γ_{25}') (see Fig. 2). We have shown the band structures of LiAlSi in all three crystal structures at a reduced volume ($S_{\text{av}}=2.35$ a.u.) in Figs. 13–15. Figures 13 and 14 show that $\text{Al}\square\text{SiLi}$ (I) goes to the metallic phase at a larger volume than predicted for the structure II. It was stated earlier (Sec. III) that the band structures of the semiconducting phases depend only weakly on the position of the Li atoms. There are details, however, where the Li positions can be noticed, and the difference in metallization volume in I and II reflects such a case. The X_1^c state, the conduction-band minimum, has a particularly large probability amplitude on site B , whereas the next higher state

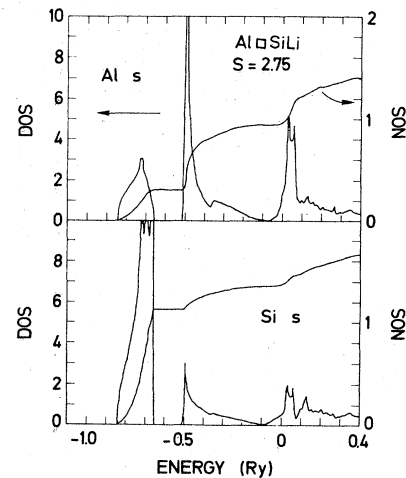


FIG. 8. $\text{Al}\square\text{SiLi}$ (I). Al- s and Si s partial DOS. $S_{\text{av}}=2.75$ a.u.

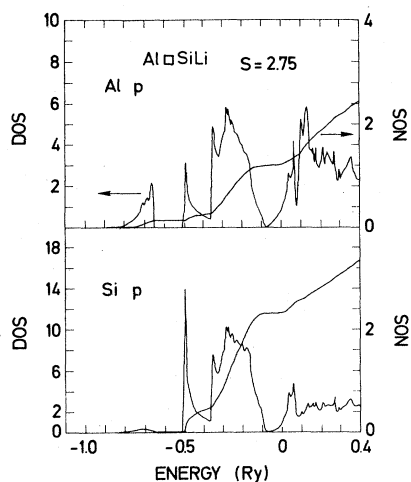


FIG. 9. AlSiLi (I). Al p and Si p partial density-of-states functions.

(X_3^c) has a large (s -like) amplitude on position D . Quantitatively this is given in the listing of the angular momentum decomposition¹⁸ in Table II. Furthermore, the actual amplitudes can be compared to those on the atomic and empty sites in GaAs.^{19,10} Thus, the X_1^c level¹⁴ will be sensitive to the occupancy, i.e., whether site B is empty as in structure I or whether an attractive Li potential is located at this place. Due to orthogonality requirements for the s states, it follows that the X_1^c level is located at a higher energy in structure II than in structure I. Consequently, the gap closes at a larger volume for LiAlSi in structure I than for the compound in structure II. Structure I metalizes very easily; the transition in fact occurs at $S_{av} = 2.65$ a.u.

It is interesting to notice that the band structure of AlSiLi (III) for the compressed lattice (Fig. 15) resembles those of structures I and II considerably more than is found for volumes around equilibrium (Figs. 3–5). Under compression s and p electrons are “squeezed” out of the Al and Si spheres into the vacancy and the Li sphere. This implies that structures I and II become more and more metallic with increasing pressure. Structure III, on the other hand, is metallic at $P = 0$. As stated earlier,

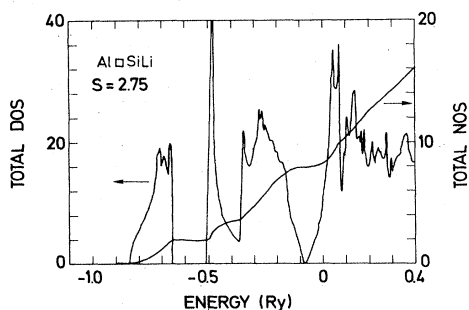


FIG. 10. AlSiLi (I). Total density of states.

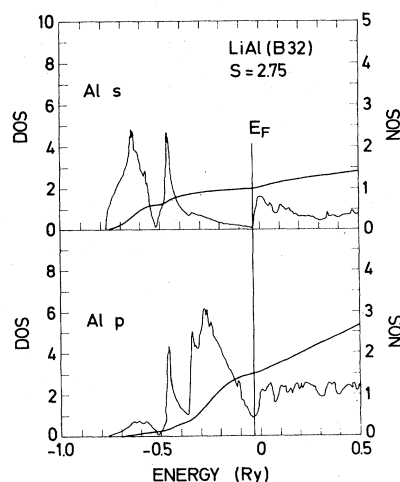


FIG. 11. Al s and Al p DOS and NOS for LiAl (B32) at the same volume, $S_{av} = 2.75$ a.u., as AlSiLi (I) (Fig. 8). (The equilibrium lattice constant of LiAl corresponds to $S_{av} = 2.95$ a.u., Ref. 2.)

Al and Si have in this structure relative positions which favor metallic bonding. Li and Al do, however, occupy zinc-blende positions, but they do not have the proper electronic configurations for formation of strong covalent bonds. This situation changes under compression, where electrons are transferred to Li. Calculations show that they essentially have p character. We show in Fig. 16 the number¹⁸ of Li p electrons as functions of the volume (expressed in terms of the average atomic-sphere radius, S_{av}). In particular, for LiAlSi -III we find that $n_p(\text{Li})$ becomes very large when the volume is reduced. At $S_{av} \approx 1.85$ a.u. there are as many p electrons in the Li sphere as in the sphere on the silicon site. Simultaneously, the state at the top of the valence band at Γ becomes predominantly of Li p character—in LiAlSi -I and -II it is a Si p state. At this large compression, $P \approx 4.8$ Mbar, a gap opens up in the band structure of LiAlSi -III, i.e., a pressure-induced metal-to-insulator transition occurs; see Fig. 17.

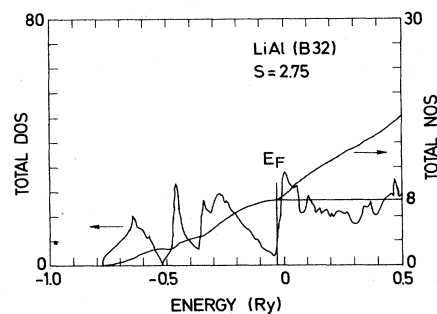


FIG. 12. LiAl . Total DOS and NOS ($S_{av} = 2.75$ a.u.).

TABLE II. $\text{AlLiSi}\square$ (II), $S_{\text{av}}=2.80$ a.u.: angular momentum decomposition of the probability amplitude in selected states. The three numbers for each state correspond to the s , p , and d orbitals in that order.

State	E (mRy)				
		A Al	B Li	C Si	D \square
Γ_{15}^v ^a	-110.77	0.0000	0.0000	0.0000	0.0000
		0.1133	0.0712	0.6047	0.0000
		0.1242	0.0051	0.0211	0.0604
Γ_1^c	29.33	0.3943	0.1194	0.4849	0.0012
		0.0001	0.0001	0.0001	0.0000
		0.0000	0.0000	0.0000	0.0000
X_1^c	-74.14	0.0000	0.4061	0.0962	0.0000
		0.1604	0.0000	0.0000	0.0518
		0.1072	0.0030	0.1182	0.0571
X_3^c	-64.00	0.2000	0.0000	0.0000	0.3575
		0.0000	0.0257	0.0864	0.0000
		0.0948	0.0826	0.1412	0.0118
X_5^v	-300.22	0.0000	0.0000	0.0000	0.0000
		0.3053	0.1574	0.4140	0.1122
		0.0039	0.0016	0.0041	0.0015
L_1^c	-52.12	0.2443	0.0523	0.2364	0.1310
		0.0463	0.1023	0.0313	0.0082
		0.0570	0.0049	0.0798	0.0062
L_3^v	-173.73	0.0000	0.0000	0.0000	0.0000
		0.2918	0.0196	0.5034	0.0251
		0.0348	0.0555	0.0202	0.0497

^aCorresponds to Γ_{25}' in Si (Fig. 2).

V. TOTAL-ENERGY CALCULATIONS

The total energies were calculated for all three structures I, II, and III of LiAlSi for varying volume. As follows from Fig. 18, we find that at zero pressure, structure I has the lowest energy among those examined. This (semiconducting) phase represents, according to Ref. 3, the observed structure of LiAlSi . The calculated equi-

librium volume, Fig. 18, corresponds to $S_{\text{av}}=2.75$ a.u., i.e., in excellent agreement with experiment,² $S_{\text{av}}=2.7588$ a.u. The small vertical bars on the total-energy curves for structures I and II indicate the volumes at which the insulator-metal transition is predicted to occur. Figure 16 further shows that for volumes smaller than that corresponding to $S_{\text{av}}=2.4$ a.u. the phase referred to as III (Table I) has the lowest energy. If we only consider the

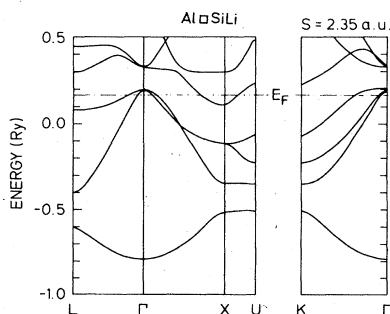


FIG. 13. LDA band structure of $\text{Al}\square\text{SiLi}$ (I) at a reduced volume ($S_{\text{av}}=2.35$ a.u.)

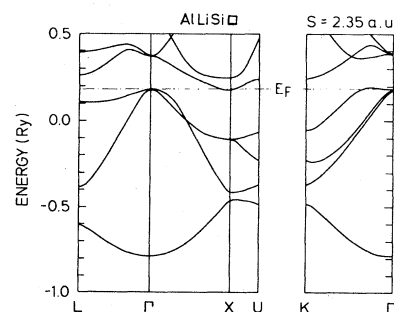


FIG. 14. Band structure of compressed $\text{AlLiSi}\square$ (II). $S_{\text{av}}=2.35$ a.u.

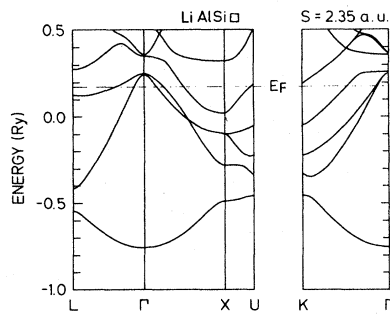


FIG. 15. Band structure of compressed LiAlSi (III). $S_{av}=2.35$ a.u.

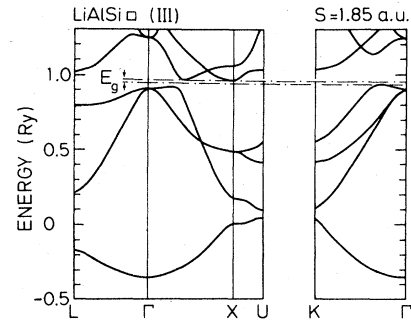


FIG. 17. Calculated LDA band structure of compressed LiAlSi in structure III (see Table I). ($S_{av}=1.85$ a.u., calculated pressure $P=5.8$ Mbar.)

three structures of Table I, our calculations predict that LiAlSi should undergo a first-order structural phase transition from I to III at a pressure of ≈ 550 kbar. The pressure-volume relation for $\text{Al}\square\text{SiLi}$ is given by Fig. 19, and in Fig. 20 we show the bulk modulus versus volume. At the equilibrium volume, $B \approx 560$ kbar according to our calculation. This value is larger than that for LiAl (415 kbar, see Ref. 2) but smaller than the value for Si (980 kbar). This again ties in with the previously noted trend in strength of the covalent bonding in the series $\text{Si} \rightarrow \text{LiAlSi} \rightarrow \text{LiAl}$. The same trend is found when the equilibrium lattice constants are considered: For Si, $S_{av}=2.526$ a.u.; for LiAl, $S_{av}=2.95$ a.u.; and $\text{Al}\square\text{SiLi}$ (I) lies between— $S_{av}=2.76$ a.u. (The lattice constants corresponding to these radii are $a=5.430$ Å, 6.341 Å, and 5.932 Å, respectively.)

VI. CHARGE DISTRIBUTIONS

The most direct way of examining the nature of the bonding consists of a calculation of the spatial distributions of the electrons in the crystal. The LMTO method is usually employed in the atomic-sphere approximation (ASA) or in a muffin-tin approximation. In both cases the charge distributions are made spherically symmetric inside spheres. Although these approximations have proved to be sufficiently accurate for many purposes, it is, however, obvious that information about directional bonds is lost by the averaging procedure. We have therefore developed²⁰ a simple method of calculating the non-spherical charge distributions in terms of the so-called "pseudo-muffin-tin" orbitals.⁸ In the interstitial regime, this density is the full (nonspherical) density, and it can conveniently be represented as a Fourier series.²⁰ From such calculations we have already² demonstrated the qualitative similarities between the Al—Al bonds in LiAl and

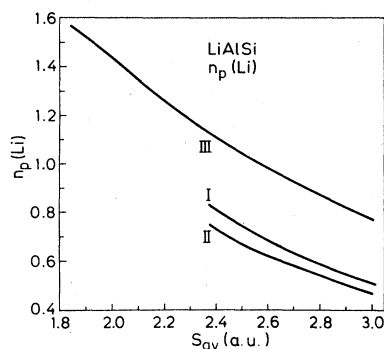


FIG. 16. Number of p electrons (see also Ref. 18) in the sphere located around the Li sites in LiAlSi-I, -II, and -III as functions of the average atomic-sphere radius S_{av} . Structure I is the one which is stable at $P=0$ and semiconducting. Structure III is metallic for pressures below ≈ 4.8 Mbar but undergoes, according to the present calculations, a transition into a semiconducting phase for higher pressures. Among the three structures examined here, III is the one which is stable at high pressures, $S_{av} < 1.88$ a.u.

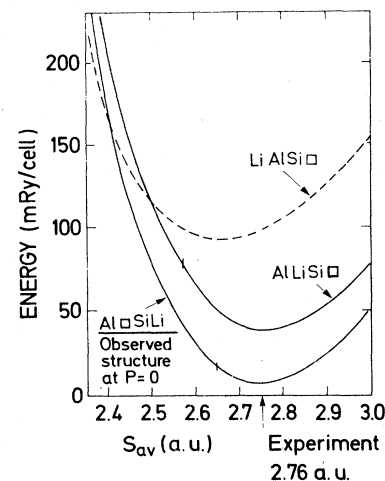


FIG. 18. Calculated total energies of LiAlSi in structures I, II, and III as functions of volume [expressed in terms of the atomic-sphere radius S_{av} (see Ref. 13)]. The small vertical bars indicate the values of S_{av} , below which I and II are metallic.

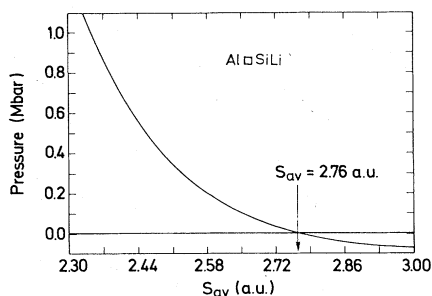


FIG. 19. Calculated total pressure of $\text{Al}\square\text{SiLi}$ (I) vs S_{av} .

the Si—Si bonds in Si. Here, we show (Fig. 21) the pseudo-MTO density in a (110) plane. Clearly, covalent bonds exist between the Al and Si sites. The maxima of the density (5) in these bonds are somewhat smaller than those in Si (Fig. 22) (8), but larger than in LiAl (Ref. 2, ≈ 3.5). These densities are given in units of $10^{-2} \times [\text{number of electrons}/(\text{bohrs})^3]$.

A further illustration is given in terms of the three-dimensional plot Fig. 23. The “mountain peaks” represent the Al—Si bond-charge maxima in $\text{Al}\square\text{SiLi}$ (I).

The charge distribution calculations thus essentially confirm the original chemical picture¹ of the bonding. The numerical values obtained for the densities again express the trends referred to previously, i.e., the Si bonds being strong, the Al—Al bonds in LiAl the weakest and the Al—Si-covalent-bond strength lying in between.

As noted in Sec. IV, we find that the structure III becomes insulating at very large pressures. The Li and Al atoms occupy sites which are favorable for the formation of sp^3 bonds; but at low pressures the number of electrons are not sufficient at these sites for such bonding. Under pressure, however, the situation is changed; s and p electrons are expelled from Si to Li and bonds of strongly covalent character form between Li and Al. This is illustrated by the density contour plot, Fig. 24. A maximum in bond charge is clearly found between Li and Al. We have not searched for an (expected) insulator-metal transition at very high pressures.

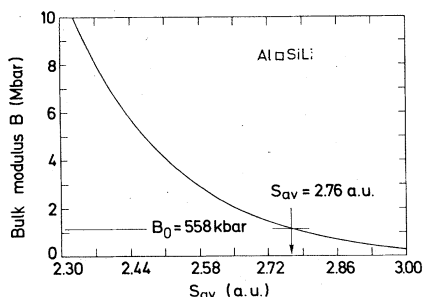


FIG. 20. Volume dependence of the theoretical bulk modulus B of $\text{Al}\square\text{SiLi}$ (I).

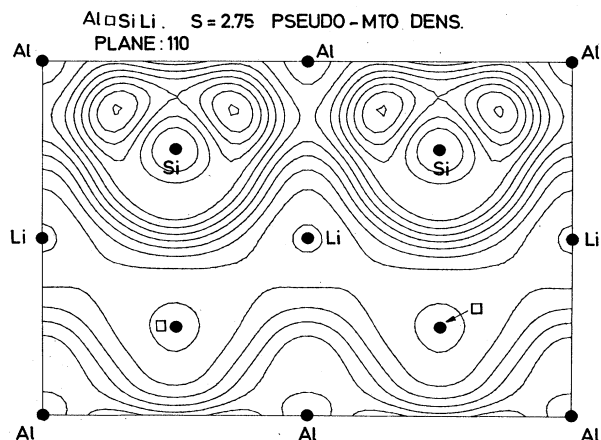


FIG. 21. Pseudo-MTO electron density contours in $\text{Al}\square\text{SiLi}$ (I) in a (110) plane. The value of S gives the atomic-sphere radius in bohrs.

VII. CONCLUSION

The present self-consistent band-structure calculations have shown that LiAlSi at zero pressure assumes a structure in which Al and Si form a zinc-blende substructure and the Li-Al arrangement is equivalent to the NaCl structure.²¹ This, as well as the calculated equilibrium volume, agrees with observations. Furthermore, the band structure and the nature of the bonding in $\text{Al}\square\text{LiSi}$ (I) are extremely similar to those of pure Si. This, and the results of the calculations of the nonspherical charge distributions, confirm the original model suggested by Zintl and Brauer.¹ The Li $2s$ state is (to some extent) transferred to Al which then forms covalent sp^3 bonds to

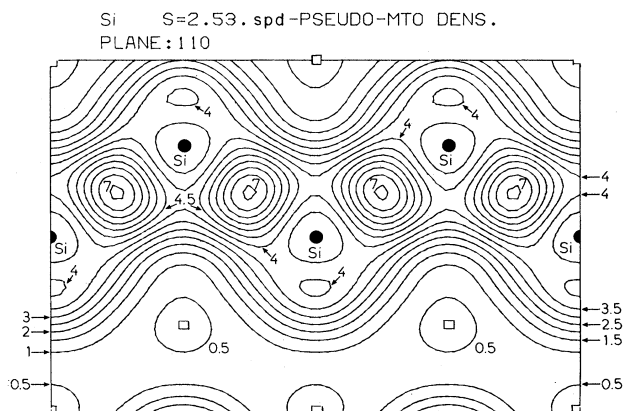


FIG. 22. Pseudo-MTO density contours in a (110) plane of Si. (The label spd indicates that s , p , and d partial waves are included.) The numbers labeling the contours give the density in $10^{-2} \times [\text{number of electrons}/(\text{bohr})^3]$.

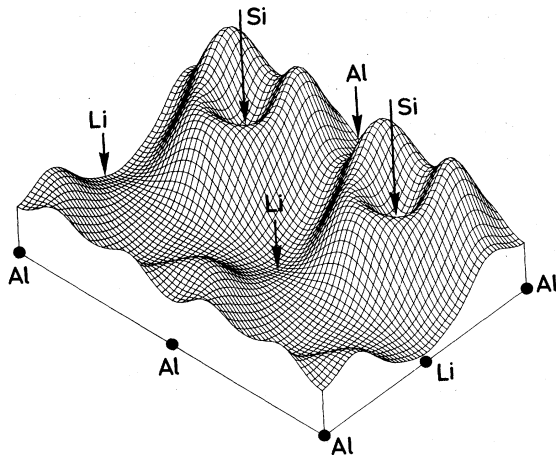


FIG. 23. Pseudo-MTO density plot for a (110) plane of AlSiLi (I). The largest maxima represent the Al—Si covalent bonds.

Si. Three possible structures were considered here. In two of these, LiAlSi is predicted to be semiconducting at zero pressure, and in the third it is metallic. The two semiconducting phases become metallic under compression; structure I at $P \approx 100$ kbar, i.e., a moderate pressure. For large compressions the third structure considered here (III) has the lowest energy. For large compressions, $P > 4.8$ Mbar, LiAlSi in this structure is predicted to un-

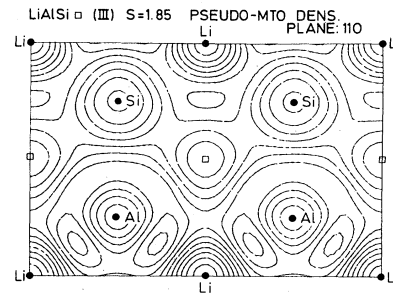


FIG. 24. Pseudo-MTO density contours of LiAlSi (III) at $P=5.8$ Mbar (calculated), corresponding to $S_{av}=1.85$ a.u. Bonds of covalent character have formed between Li and Al.

dergo a transition from a metallic into a semiconducting phase with covalent bonds forming between Li and Al. We have not examined all possible crystal structures, but this result shows that at least one structural phase transition must occur in LiAlSi under pressure.

ACKNOWLEDGMENTS

The present study was stimulated by the current experimental work carried out at the Max-Planck-Institute by H. G. von Schnering and R. Nesper, who we thank for many helpful discussions.

¹E. H. Zintl and G. Brauer, *Z. Phys. Chem. Abt. B* **20**, 245 (1933).

²N. E. Christensen, *Phys. Rev. B* **32**, 207 (1985).

³H.-U. Schuster, H.-W. Hinterkeuser, W. Schäfer, and G. Will, *Z. Naturforsch.* **31B**, 1540 (1976). R. Nesper and H. G. von Schnering (private communication).

⁴P. Hohenberg and W. Kohn, *Phys. Rev.* **136**, B864 (1964).

⁵W. Kohn and L. J. Sham, *Phys. Rev.* **140**, A1133 (1965).

⁶L. Hedin and B. I. Lundqvist, *J. Phys. C* **4**, 2064 (1971).

⁷U. von Barth and L. Hedin, *J. Phys. C* **5**, 1629 (1972).

⁸O. K. Andersen, *Phys. Rev. B* **12**, 3060 (1975).

⁹D. Glötzel, B. Segall, and O. K. Andersen, *Solid State Commun.* **36**, 403 (1980).

¹⁰G. B. Bachelet and N. E. Christensen, *Phys. Rev. B* **31**, 879 (1985).

¹¹N. E. Christensen, *Phys. Rev. B* **30**, 5753 (1984).

¹²D. R. Hamann, *Phys. Rev. Lett.* **42**, 662 (1979).

¹³The atomic sphere radius is given by $4(4\pi/3)S_{av}^3 = a^3/4$. The band structure of Si is calculated for a structure containing four atoms (four Si atoms plus two "empty spheres") per fcc Bravais lattice point (cf. Fig. 1).

¹⁴For convenience we label the states in AlSiLi with those used for Si. This makes the comparison to Si easier, but does not, of course, correspond to the correct symmetry.

¹⁵The total energy does of course depend on the position of the Li atom as follows from Sec. IV. In a "frozen-potential" approach covalent and Madelung contributions to structural energy differences can be separated conveniently (Ref. 16).

¹⁶O. K. Andersen and N. E. Christensen (unpublished).

¹⁷In the present LMTO calculations we have decided always to use atomic spheres of the same size on all sites, i.e., $S_A = S_B = S_C = S_D = S_{av}$.

¹⁸Due to the ambiguity in division of space into "Si regions," "Al regions," etc., site-projected density of states are not precise concepts. Also quantities such as "charge transfer" cannot be defined in a physically meaningful way. Thus, we cannot with a particular choice of atomic-sphere radius ratios (see Ref. 17) calculate the number of *s* and *p* states at each site (n_p, n_s), and conclude from the ratio n_p/n_s whether sp^3 hybrids have formed or not.

¹⁹N. E. Christensen and G. B. Bachelet, in *Proceedings of the 17th International Conference on the Physics of Semiconductors, San Francisco, 1984*, edited by J. D. Chadi and W. A. Harrison (Springer, Berlin, 1985), p. 1009.

²⁰N. E. Christensen, *Phys. Rev. B* **29**, 5547 (1984).

²¹Note that simultaneously Li and Si also form a zinc-blende substructure.